

Supporting Information for

Modeling Electrochemical Behavior and Interfacial Junction Profiles of Bipolar Membranes at Solar Flux Relevant Operating Current Densities

Meng Lin^{a}, Ibadillah A. Digdaya^b, Chengxiang Xiang^{b*}*

*^a Department of Mechanical and Energy Engineering, Southern University of Science
and Technology, Shenzhen 518055, China*

*^b Liquid Sunlight Alliance, and Division of Engineering and Applied Science,
California Institute of Technology, Pasadena, California 91125, United States*

*To whom correspondence should be addressed: cxx@caltech.edu, linm@sustech.edu.cn

Table S1. Diffusion coefficients of each species in aqueous solution.

Species	Diffusion coefficient
H^+	$9.31 \times 10^{-5} \text{ cm}^2 \text{ s}^{-1}$
OH^-	$5.26 \times 10^{-5} \text{ cm}^2 \text{ s}^{-1}$
K^+	$1.95 \times 10^{-5} \text{ cm}^2 \text{ s}^{-1}$
HPO_4^{2-}	$0.7 \times 10^{-5} \text{ cm}^2 \text{ s}^{-1}$
H_2PO_4^-	$0.85 \times 10^{-5} \text{ cm}^2 \text{ s}^{-1}$
SO_4^{2-}	$1.065 \times 10^{-5} \text{ cm}^2 \text{ s}^{-1}$
NaSO_4^-	$0.618 \times 10^{-5} \text{ cm}^2 \text{ s}^{-1}$
Cl^-	$2.03 \times 10^{-5} \text{ cm}^2 \text{ s}^{-1}$
f_{water}	0.215 (fitted value)
f_{water} (buffer case)	0.158 (fitted value)
θ in Bruggeman model	1.5 (default value)
θ (buffer case)	K^+ , H_2PO_4^- and HPO_4^{2-} were fitted as 2.1, 1.0 and 1.0, and kept 1.5 for all other species

Table S2 Parameters used for calculation of dielectric constant.³

Parameters	Values/Equations
Vacuum permittivity (ϵ_0)	$8.85e \times 10^{-12}$ (F/m)
Water permittivity (ϵ_{water})	$\epsilon_{\text{water}} = (2.313 \times 10^{-2} - 3.475 \times 10^{-5} T)^{-1} \epsilon_0$
Membrane permittivity (ϵ_{mem})	$\epsilon_{\text{mem}} = 2.21 \epsilon_0$
Fitting permittivity (ϵ_{fit})	$\epsilon_{\text{fit}} = \epsilon_0 (0.48 + 4.55 f_{\text{water}}) / (0.27 f_{\text{water}} - 2.39) / ((1 - f_{\text{water}}) f_{\text{water}})^3$
Overall dielectric constant (ϵ)	$\epsilon = (f_{\text{water}} / \epsilon_{\text{water}} + (1 - f_{\text{water}}) / \epsilon_{\text{mem}} + 1 / \epsilon_{\text{fit}})^{-1}$ ^{3,4}

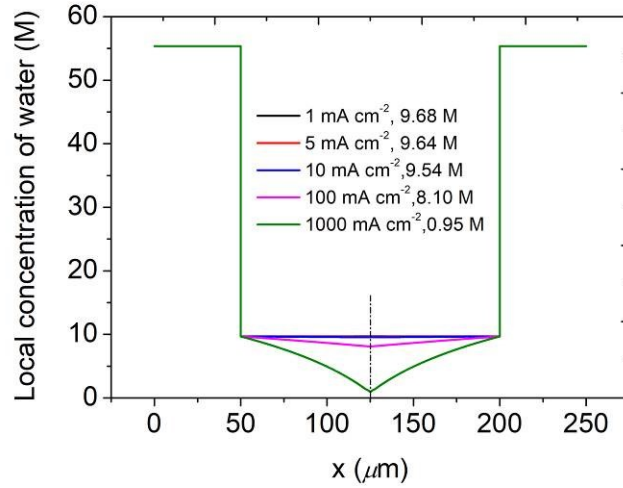


Figure S1. Local water concentration profiles and junction concentration values as a function of operational current density.

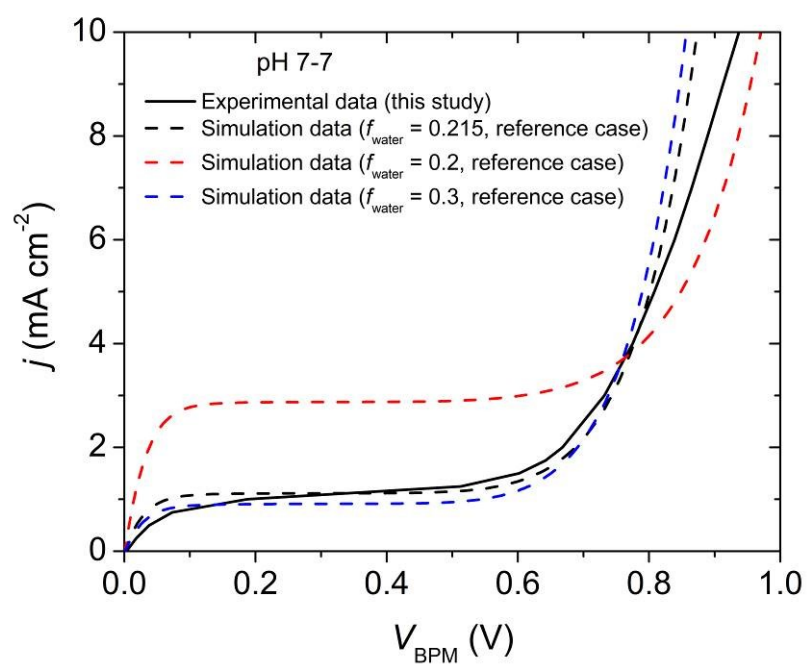


Figure S2. The IV curves for the cases with different water fractions.

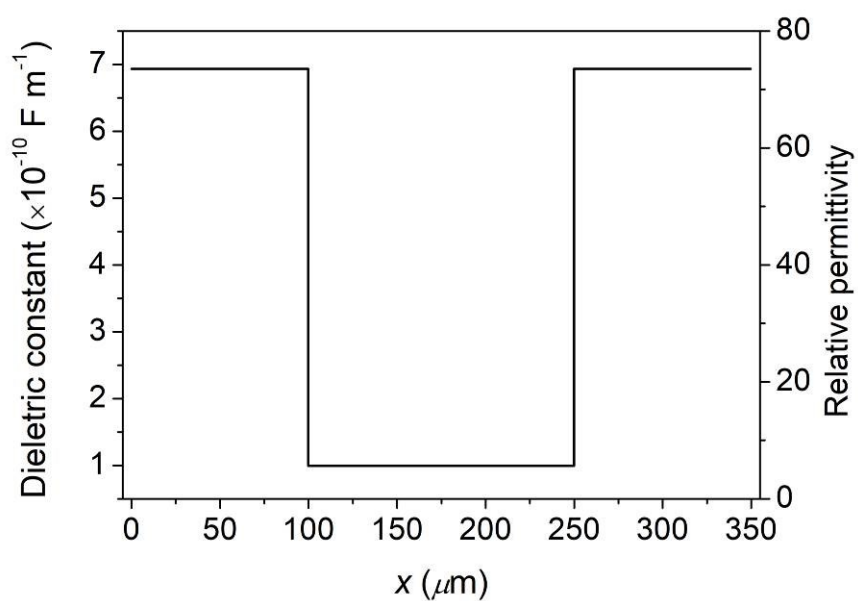


Figure S3. Dielectric constant and relative permittivity along x axis.

Table S3. Summary of governing equations. The total number of governing PDEs are 10 for pH 0/pH 14 case, 12 for pH 7/pH 7 case, and 16 for phosphate buffer case.

Nernst-Planck equations:

pH 0/pH 14 case: $i = H_3O^+, OH^-, K^+$, and Cl^- ;

pH 7/pH 7 case: $i = H_3O^+, OH^-, K^+, SO_4^{2-}$, and $NaSO_4^-$;

phosphate buffer case: $i = H_3O^+, OH^-, K^+, HPO_4^{2-}, H_2PO_4^-, NaHPO_4^-$, and NaH_2PO_4

$$N_i = -D_i \frac{dc_i}{dx} + nD_i c_i \frac{FE}{RT} + D_i c_i \frac{dc_{H_2O}}{dx} + 0.5D_i c_i \frac{d \ln \left(\frac{k_-^E}{k_+^E} \right)}{dx} \quad (i = H_3O^+, OH^-) \quad (S1)$$

$$N_i = -D_i \frac{dc_i}{dx} + nD_i c_i \frac{FE}{RT} + D_i c_i \frac{dc_{H_2O}}{dx} \quad (i \neq H_3O^+, OH^-) \quad (S2)$$

$$\frac{dN_i}{dx} = R_i \quad (S3)$$

Possions' equations:

$$\frac{d(\varepsilon E)}{dx} = F \sum_i c_i \quad (S4)$$

$$-\frac{d\phi}{dx} = E \quad (S5)$$

Table S4. Reaction constants used in this study.³

Parameters	Values
k_{+1}^0 ³	$3.67 \times 10^{-10} \text{ m}^3\text{s}^{-1}\text{mol}^{-1}$
k_{-1}^0 ³	$1.11 \times 10^8 \text{ m}^3\text{s}^{-1}\text{mol}^{-1}$
k_{+2}^0 ³	$83.9 \text{ m}^3\text{s}^{-1}\text{mol}^{-1}$
k_{-2}^0 ³	$2.13 \times 10^7 \text{ m}^3\text{s}^{-1}\text{mol}^{-1}$
k_{+3}^0 ³	$1.8 \times 10^5 \text{ m}^3\text{s}^{-1}\text{mol}^{-1}$
k_{-3}^0 ³	$2.15 \times 10^7 \text{ m}^3\text{s}^{-1}\text{mol}^{-1}$
pKa for R4 ⁵	6.62 at 1.0 M
k_{+4}	10^2 s^{-1}
K_5 ⁶	0.483 M
k_{5+}	10^2 s^{-1}

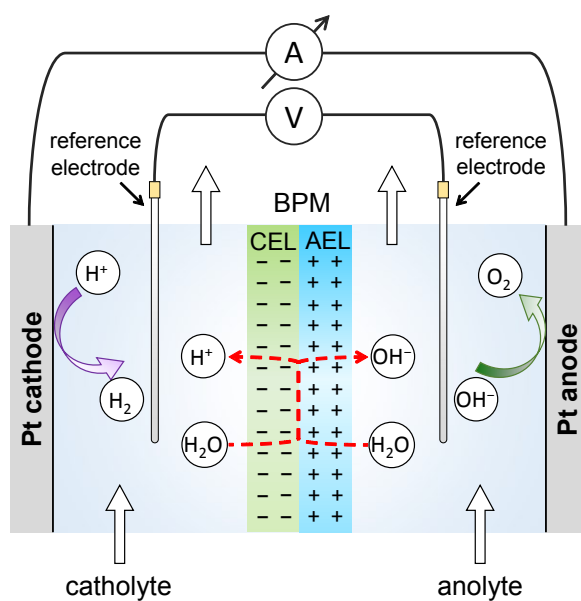


Figure S4. Schematic illustration of the experimental setup consisting of a Pt cathode, a catholyte compartment, a BPM, an anolyte compartment and a Pt anode. BPM voltages were measured in a 4-wire sensing mode. Electrical currents were applied at the cathode and at the anode, and the voltage differences between the two reference electrodes were measured.

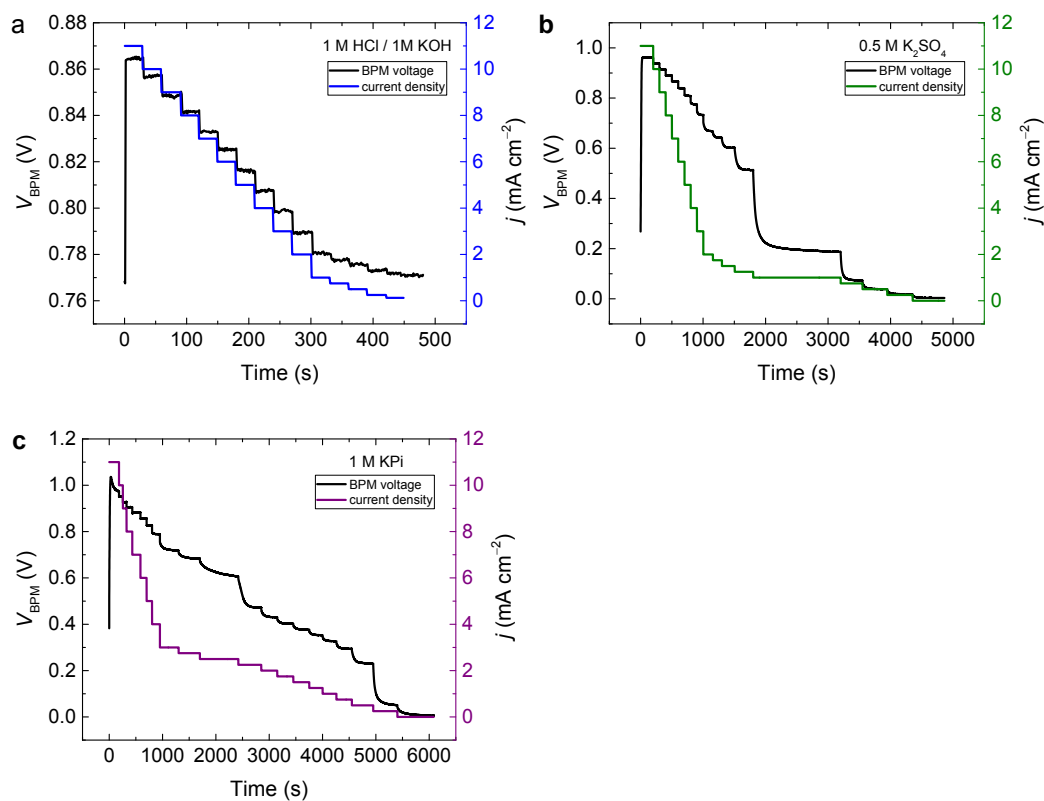


Figure S5. BPM voltage measurements using multistep chronopotentiometry mode from high current density (11 mA cm^{-2}) to low current density (0 mA cm^{-2}) for (a) 1 M HCl and 1 M KOH (pH 0/pH 14), (b) 0.5 M K_2SO_4 , and (c) 1 M potassium phosphate buffer (containing 0.54 M K_2HPO_4 and 0.46 M KH_2PO_4). The voltage at each applied current density was recorded once the voltage stabilized to ensure that the BPM voltage was not underestimated.

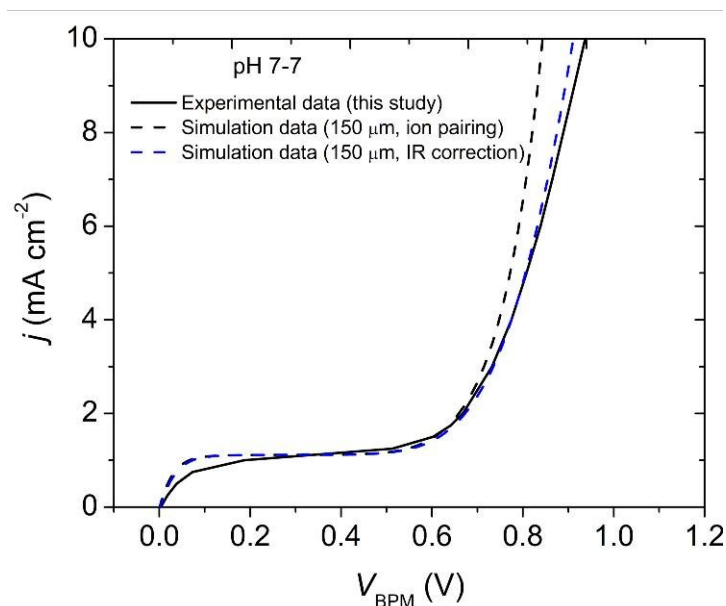


Figure S6. IR corrected IV curve for the pH7/pH7 case.

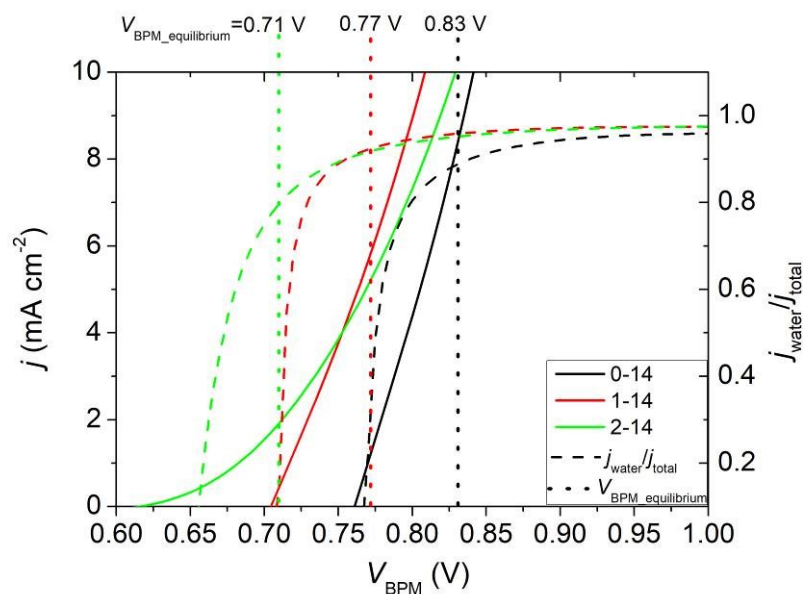


Figure S7. The total current density (left y-axis, solid lines) and fraction of current density due to water dissociation (right y-axis, dashed lines) for different combination of pHs (0-14, 1-14, 2-14). The equilibrium potentials are indicated by colored dots. The pHs at the two sides of BPM are created numerically by changing the concentration of HCl (CEM side) and KOH (AEM side). This verifies the water dissociation has been activated before the equilibrium potential.

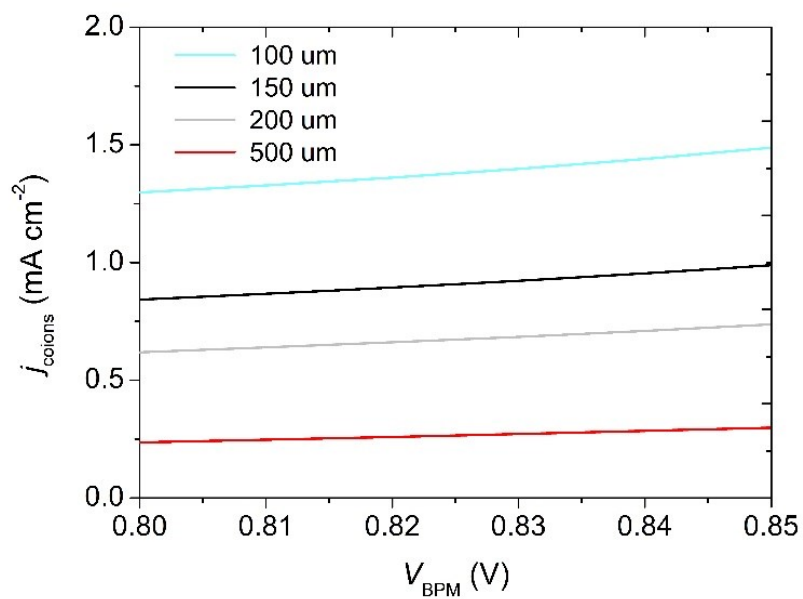


Figure S8. Co-ion partial current density as a function of V_{BPM} for various membrane thickness.

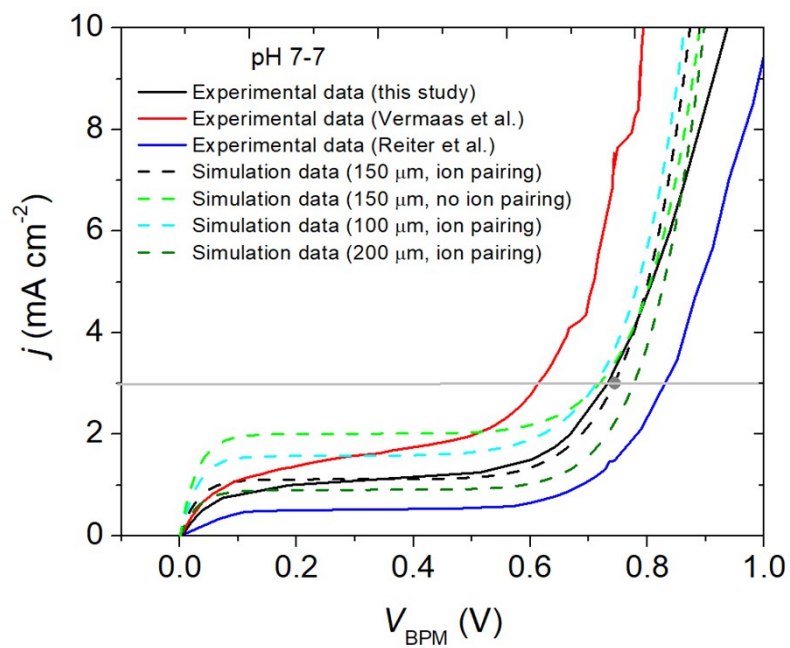


Figure S9. Effect of membrane thickness on the electrochemical behavior of the BPM. Note that the AEL and CEL are assumed to be identical in thickness.

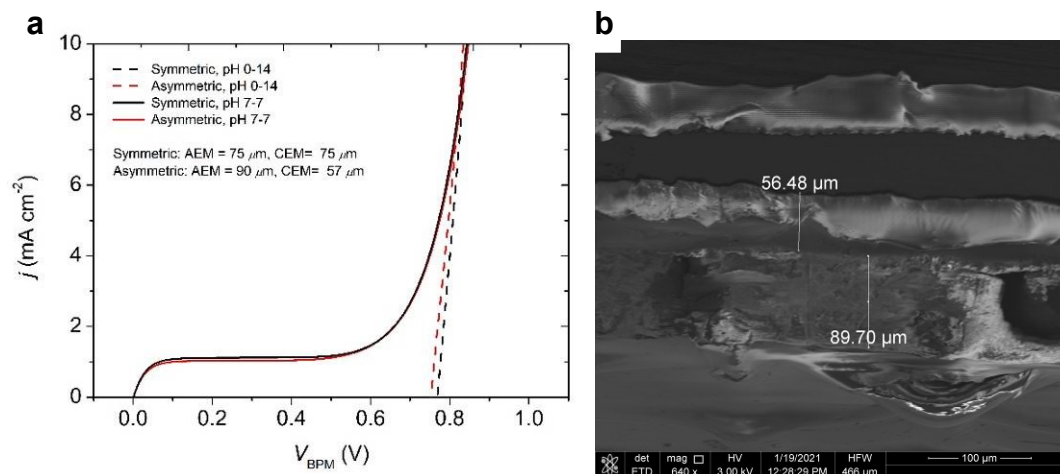


Figure S10: (a) Effect of asymmetric membrane thickness on the electrochemical behavior of BPM for both 0-14 and 7-7 cases. The asymmetric dimensions are obtained experimentally. (b) Cross-section scanning electron microscopy (SEM) image of the Fumasep BPM, showing asymmetric thickness of anion exchange layer (89.7 μm) and cation exchange layer (56.48 μm)

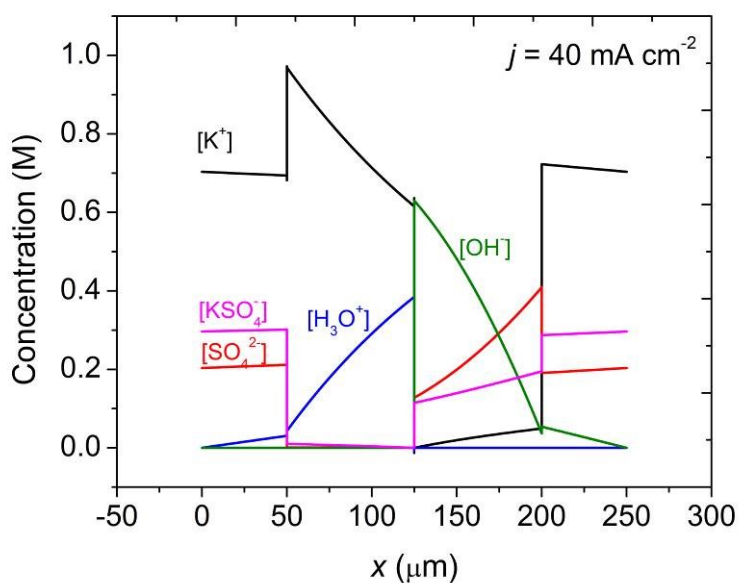


Figure S11. The concentration profile of H_3O^+ , OH^- and other co-ions across the BPM at different pKa of the WD catalyst at a current density of 40 mA cm^{-2} .

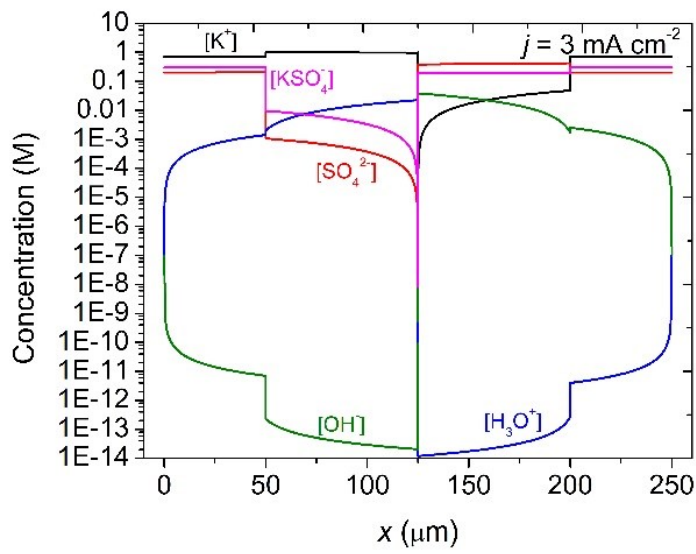


Figure S12. The concentration profile of H_3O^+ , OH^- and other co-ions across the BPM at a current density of 3 mA cm^{-2} .

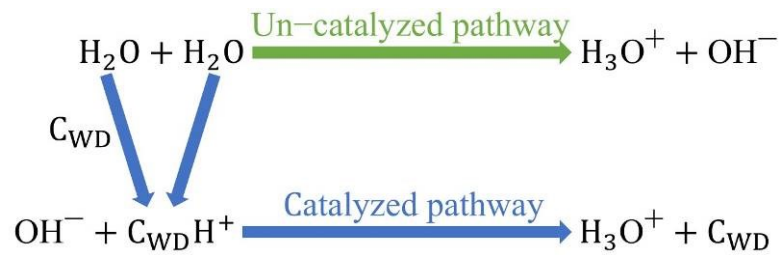


Figure S13. Schematic for the catalyzed and uncatalyzed pathways for water dissociation reactions at CL.

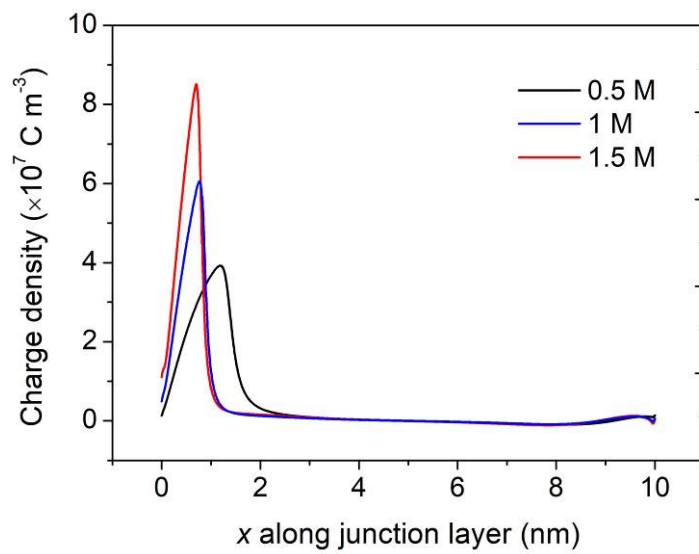


Figure S14. Charge density along the BPM junction layer for different fixed charge densities.

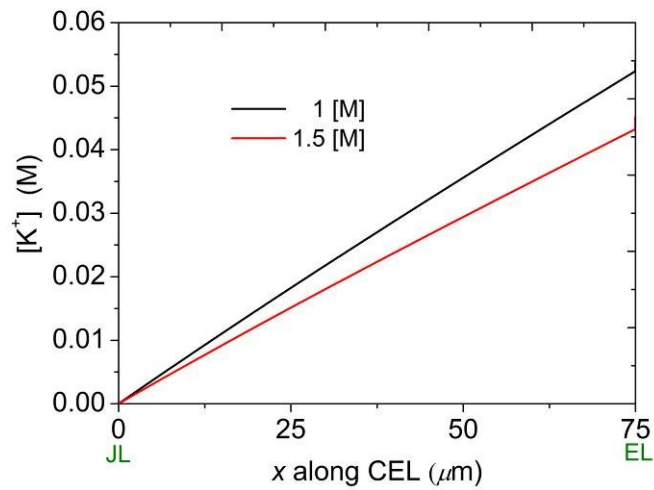


Figure S15. The K^+ concentration at CEL under different fix charge density at a current density of 3 mA cm^{-2} .

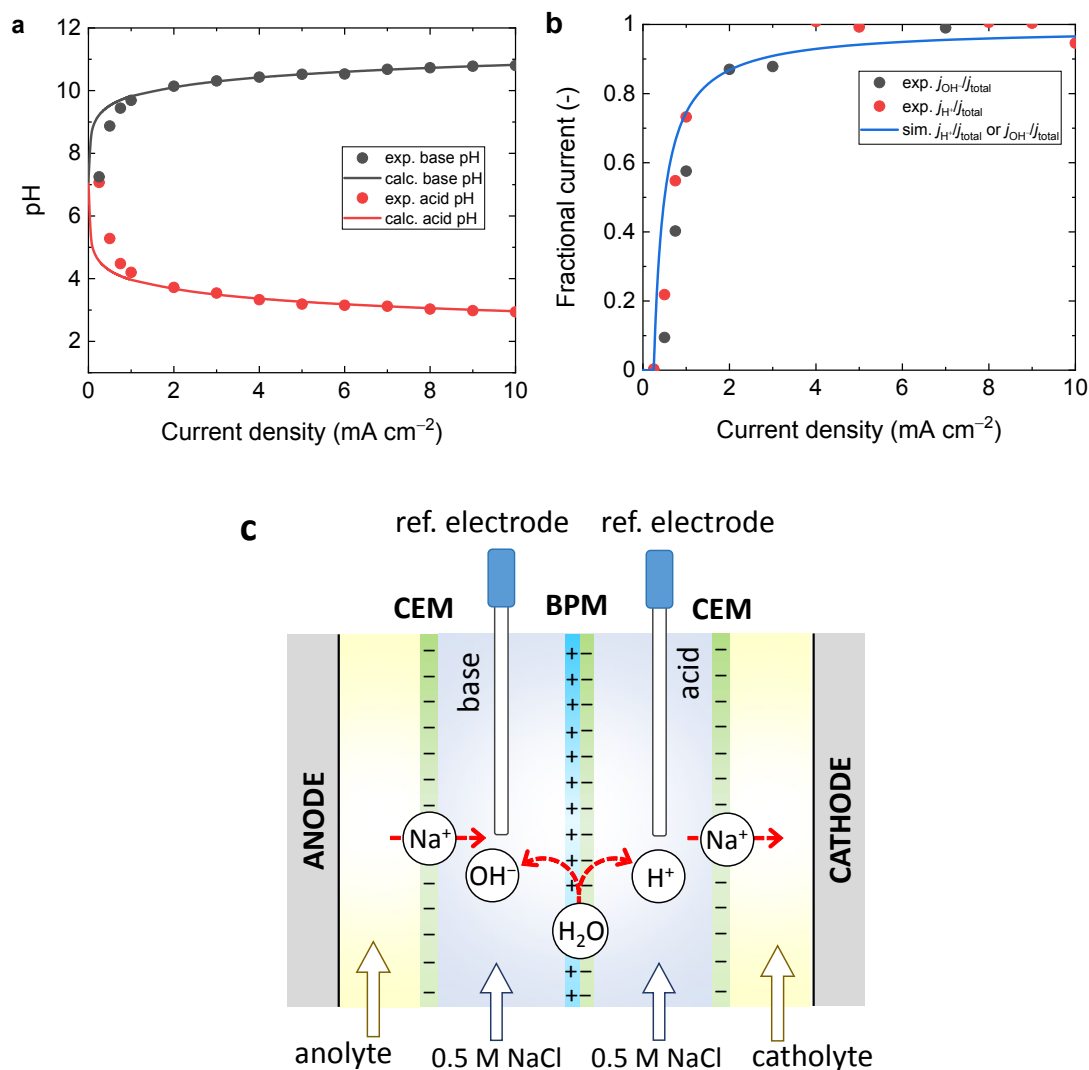


Figure S16. (a) The experimental (exp.) and calculated (calc.) acid and base pH as a function current density for a 0.5 M NaCl solution and a BPM with an active area of 0.95 cm². Calculated values assumed 100% generation rate of protons and hydroxides ($G_{H^+}, G_{OH^-} = I/(nF)$, where I is the absolute current, n is the number of participating electron (1) and F is the Faraday's constant) at the BPM. The experimental data were determined from pH measurements of the output solutions. (b) Experimental and simulated (sim.) values of partial current density carried by H⁺ and OH⁻ as a function of the total current density. Experimental data were determined by dividing the generated H⁺ and OH⁻ as measured from the solutions pH with the calculated values assuming 100% generation of protons and hydroxides at the BPM. The low fractional current of H⁺ and OH⁻ at low current densities represent the co-ion leakage (Na⁺ and Cl⁻) due to imperfect permselectivity of the anion exchange layer (AEL) and cation exchange layer (CEL) of the BPM. (c) Experimental electrochemical setup for the pH measurements, consisting of (left to right) an anode, an anolyte compartment, an CEM, a base compartment, a BPM, an acid compartment, a CEM, a catholyte and a cathode. The anolyte and catholyte were 1 M Na₂SO₄ and the investigated solution flowing through the base and acid compartment was 0.5 M NaCl. The concentration

of Na⁺ in the acid compartment was significantly higher (0.5 M) than that of H⁺ generated at the BPM (between $\sim 10^{-7}$ and 10^{-3} for pH 7 to pH 3), and therefore the transference number was close to unity for Na⁺ across the CEM, and the transport of H⁺ escaping from the acid compartment to the catholyte compartment was negligible.

References:

- 1 J. Newman and K. E. Thomas-Alyea, *Electrochemical Systems, 3rd Edition*, 2004.
- 2 D. L. Parkhurst and C. A. J. Appelo, *Model. Tech. B.* 6, , DOI:Rep. 99-4259.
- 3 N. Craig, *UC Berkeley Electron. Theses Diss.*, 2013, 116.
- 4 F. E. Critchfield, J. A. Gibson and J. L. Hall, *J. Am. Chem. Soc.*, 1953.
- 5 A. A. Green, *J. Am. Chem. Soc.*, 1933, **55**, 2331–2336.
- 6 E. J. Reardon, *J. Phys. Chem.*, 1975, **79**, 422–425.